

APPROVED FOR PUBLICATION

AAEC/E295

AAEC/E295



**AUSTRALIAN ATOMIC ENERGY COMMISSION**  
**RESEARCH ESTABLISHMENT**  
**LUCAS HEIGHTS**

**TIME DEPENDENT  $^{237}\text{Np}$ ,  $^{235}\text{U}$  AND  $^{239}\text{Pu}$  FISSION RATES IN A THORIUM  
ASSEMBLY DURING THE INTERVAL 0 TO 200 ns USING A  
PULSED  $^9\text{Be}(d,n)$  SOURCE PART II – THEORY**

by

S. P. MOO \*

M. T. RAINBOW

A. I. M. RITCHIE

\* University of Tasmania, Hobart

February 1974

ISBN 0 642 99612 1

APPROVED FOR PUBLICATION



AUSTRALIAN ATOMIC ENERGY COMMISSION

RESEARCH ESTABLISHMENT

LUCAS HEIGHTS

TIME DEPENDENT  $^{237}\text{Np}$ ,  $^{235}\text{U}$  and  $^{239}\text{Pu}$  FISSION RATES IN A THORIUM ASSEMBLY  
DURING THE INTERVAL 0 TO 200 ns USING A PULSED  $^9\text{Be}(d,n)$  SOURCE  
PART II - THEORY

by

S.P. MOO\*

M.T. RAINBOW

A.I.M. RITCHIE

ABSTRACT

Calculations are presented of the  $^{237}\text{Np}$ ,  $^{235}\text{U}$  and  $^{239}\text{Pu}$  fundamental mode fission rates in a thorium assembly based on a diffusion theory code with a  $\text{DB}^2$  leakage term. Three different thorium cross section sets derived from the ABBN set, the UKNDL68 file and the ENDF/B-II file were used in the calculations and the results compared with each other and with experimental results reported previously.

The sensitivity of the instantaneous decay constant of the fundamental mode to changes in partial cross sections is investigated.

*Note: This work has been submitted to a journal. Further details can be obtained from the authors or the Director of the Research Establishment.*

\* University of Tasmania, Hobart.

National Library of Australia card number and ISBN 0 642 99612 1

The following descriptors have been selected from the INIS Thesaurus to describe the subject content of this report for information retrieval purposes. For further details please refer to IAEA-INIS-12 (INIS: Manual for Indexing) and IAEA-INIS-13 (INIS: Thesaurus) published in Vienna by the International Atomic Energy Agency.

BUCKLING; CROSS SECTIONS; DECAY; ENERGY SPECTRA; FISSION;  
MULTIGROUP THEORY; NEPTUNIUM 237; NEUTRON BEAMS; NEUTRON  
FLUX; NEUTRON LEAKAGE; NEUTRON SOURCES; PLUTONIUM 239;  
PULSED NEUTRON TECHNIQUES; THORIUM; TIME DEPENDENCE;  
SENSITIVITY; URANIUM 235

## CONTENTS

	Page
1. INTRODUCTION	1
2. CALCULATIONAL METHOD	1
2.1 Basis of the Calculational Method	1
2.2 Energy Distribution of the Source	2
2.3 Time Dependence of the Source	2
2.4 Detector Timing Jitter	3
3. THORIUM DATA SETS	4
4. RESULTS OF CALCULATIONS	5
5. DISCUSSION	5
5.1 The $^{237}\text{Np}$ Fission Rates	5
5.2 The $^{235}\text{U}$ and $^{239}\text{Pu}$ Fission Rates	6
5.3 General	6
6. SENSITIVITY STUDIES	10
7. ACKNOWLEDGEMENTS	12
8. REFERENCES	13

Figure 1 Angle integrated neutron energy spectrum from the  $^9\text{Be}(d,n)^{10}\text{B}$  thick target reaction.

Figure 2 The group averaged (a) elastic and (b) inelastic cross sections for thorium derived from the UKNDL68 and ENDF/B-II data files.

Figure 3 Theoretical and experimental values of the fundamental mode fission rates for  $^{237}\text{Np}$  as a function of time. (a) The fundamental mode time distribution. (b) The instantaneous decay constant  $\lambda(t)$ .

Figure 4 Theoretical and experimental values of the fundamental mode fission rates for  $^{235}\text{U}$  as a function of time. (a) The fundamental mode time distribution. (b) The instantaneous decay constant  $\lambda(t)$ .

Figure 5 Theoretical and experimental values of the fundamental mode fission rates for  $^{239}\text{Pu}$  as a function of time. (a) The fundamental mode time distribution. (b) The instantaneous decay constant  $\lambda(t)$ .

CONTENTS (Cont'd.)

Figure 6 Percentage changes in the instantaneous decay constant  $\lambda(t)$  of (a)  $^{237}\text{Np}$  and (b)  $^{235}\text{U}$  fission rates for given changes in the thorium group-averaged elastic cross section.

## 1. INTRODUCTION

In a previous paper (Moo, Rainbow and Ritchie 1973) the results were reported of a series of integral pulsed neutron experiments in a thorium assembly. The experiments consisted of measuring the space dependent, time dependent fission rates of  $^{237}\text{Np}$ ,  $^{235}\text{U}$  and  $^{239}\text{Pu}$  following the injection of a short burst of fast neutrons into the centre of the assembly which was a cube of about 0.4 m side. Analysis of the data was directed mainly to the extraction of the fission rates corresponding to the fundamental three-dimensional Fourier spatial mode.

This paper presents a comparison of these experimental fundamental mode fission rates with fission rates calculated from a diffusion theory code which uses asymptotic reactor theory to describe leakage. Incorporated in the calculations are the effects of the finite width of the initial neutron pulse and smearing of the time dependent reaction rates due to timing jitter in the detector signals. Three different thorium cross section sets derived from the ABBN set (Bondarenko 1964) the UKAEA Nuclear Data Library (UKNDL68) file (Norton 1968), and the ENDF/B-II file, were used in the calculations and the results compared with each other and with experiments.

The sensitivity of the experimentally measured parameters to possible errors in the nuclear data is clearly of interest. Section 6 describes some studies in which changes in the instantaneous decay constant of the fundamental Fourier mode time distributions were noted as a function of changes in the values of group cross sections for the various neutron reactions in thorium. These changes have been limited to the energy range 300 keV to 10 MeV since the experiments were limited to the time range 200 ns after the pulse at which time most neutrons from the  $^9\text{Be}(d,n)^{10}\text{B}$  source have slowed down to about 100 keV.

## 2. CALCULATIONAL METHOD

### 2.1 Basis of the Calculational Method

The calculations were based on the time dependent multigroup diffusion theory code TENDS (Maher, Ritchie and Rainbow 1967). This code approximates leakage with a buckling term and solves the multigroup set of equations

$$\frac{1}{V_j} \frac{d\phi_j(t)}{dt} = -(D_j B^2 + \Sigma_j) \phi_j(t) + \sum_{k=1}^N \Sigma_{k \rightarrow j} \phi_k(t) + \sum_{k=1}^N \chi_j \bar{v}_k \Sigma_k^f \phi_k + S_j(t)$$

... (1)

where the symbols have their usual meaning. Time dependent fission rates corresponding to the fundamental spatial mode then take the form

$$R'(t, B^2) = \sum_{j=1}^N \sum_n^f \phi_j(t, B^2)$$

where  $\sum_n^f$  is the multigroup cross section for fission in the nuclide of interest. The quantity  $R'(t, B^2)$  can be compared, within a scale factor, with the experimentally measured fundamental spatial mode fission detector response provided there is no self shielding in the detector and provided the fundamental spatial mode of the calculation corresponds to that of the experiment.

The light loading of the fissionable material in the detectors and the low fission cross sections at the energies of present interest (100 keV to 10 MeV) make self shielding corrections in the detector negligibly small. The second condition can also be fulfilled, as has been pointed out elsewhere (Ritchie and Moo 1974), by using a time independent characteristic length for Fourier analysing the experimental spatial distributions and using the same characteristic length in calculating the buckling term to insert in the diffusion theory calculation.

## 2.2 Energy Distribution of the Source

The energy distribution of the source was taken into account explicitly in the multigroup formalism. The neutron spectrum appropriate to the thick target  ${}^9\text{Be}(d, n){}^{10}\text{B}$  reaction at a bombarding energy of 2.8 MeV was obtained in the following manner.

(a) Above 200 keV, the spectrum was derived by integrating the angle dependent neutron spectra measurements of Inada, Kawachi and Hiramoto (1968). This neutron spectrum is shown in Figure 1.

(b) At energies below 200 keV the spectrum was assumed flat and extrapolated from 200 keV to ~15 keV. This lower energy limit corresponds to neutrons emitted at threshold from the reaction that leaves  ${}^{10}\text{B}$  in the first excited state. The fraction of neutrons in the interval 200 keV to ~15 keV is about 6 per cent which is consistent with an estimate made from the thick target total yield curve and with the recent measurements of Whittlestone (1972).

## 2.3 Time Dependence of the Source

The time behaviour of the source was assumed to be Gaussian with the same width (FWHM) as that of the beam pulse measured during the experiments. The Gaussian shape was approximated in the calculation by a histogram

consisting of simple rectangular pulses. In this representation the source may be written in the form

$$s(t) = \begin{cases} h_1 & \text{for } 0 < t \leq p/n \\ h_2 & \text{for } p/n < t \leq 2p/n \\ \vdots & \\ \vdots & \\ h_n & \text{for } (n-1)p/n < t \leq p \end{cases}$$

where  $p/n$  is the duration of each rectangular pulse and  $h_i$  ( $i=1, \dots, n$ ) are the relative heights of the rectangular pulses in the histogram.

During the source pulse ( $t \leq p$ ) the group fluxes  $\phi_j(t)$  were derived from the expression

$$\phi_j(t) = \sum_{i=1}^m h_i F_j^{ip/n}(t) \quad (m-1)p/n \leq t \leq mp/n$$

where  $F_j^{ip/n}(t)$  are the group fluxes corresponding to a rectangular pulse of unit height and duration  $p/n$  in the time interval between  $(i-1)p/n$  and  $ip/n$ . The group fluxes  $\phi_j(t)$  at times after the source pulse ( $t \geq p$ ) were calculated from the values at  $t = p$  in the usual manner (Maher, Ritchie and Rainbow 1967).

#### 2.4 Detector Timing Jitter

The jitter in the timing of events from the fission detectors smears out the time dependent fission rates and introduces a systematic difference between the measured time dependence of the fission rates and those calculated in a code such as TENDS. Intrinsically, it is much more difficult to unfold from the measured time distributions the effect of detector jitter than to fold into the calculations the effect of detector jitter. The latter may be done by using an expression of the form

$$R(t, B^2) = \int_0^t G(\tau) R'(t - \tau, B^2) d\tau$$

where  $G(t)$  is the detector timing uncertainty distribution. In the calculations to be presented it was assumed that  $G(t)$  was Gaussian in shape with a standard deviation of 4.15 ns for  $^{237}\text{Np}$  and  $^{235}\text{U}$  and a standard deviation of 2.8 ns for  $^{239}\text{Pu}$ . These values are the averages of the upper and lower bounds assigned to the standard deviations from measurements of the timing uncertainty in the detectors used (Moo, Rainbow and Ritchie 1973).

### 3. THORIUM DATA SETS

Three different sources of thorium data were used. The first was the ABBN 26 group set (Bondarenko 1964) which spans the energy range from 10.5 MeV to thermal and has 14 groups above 1 keV. Cross sections in the top three groups are averaged over a fission spectrum, while the remaining cross sections are averaged over a 1/E spectrum.

The second source was a 50 group set derived from the UKNDL68 file (Norton 1968), using the local AAEC codes BOMB (Doherty 1968) and BOMBO (Clancy 1969), and covers the energy range from 10 MeV to 1.58 keV. Above 50 keV the data were averaged over an integrated fission spectrum

$$F(E) = a \int_E^{\infty} \sqrt{Z} \exp(-Z/T) dZ$$

where the parameters  $a$  and  $T$  are those relevant to  $^{235}\text{U}$  (Argonne National Laboratory 1963). Below 50 keV the data were averaged over a 1/E spectrum.

The third set was generated by the code SUPERTO (Wright et al. 1969) from the cross sections in the ENDF/B-II file. The group structure and the averaging spectrum are the same as for the UKNDL68 50 group set.

Examples of the differences between the two 50 group sets are shown in Figure 2a for the inelastic cross section and in Figure 2b for the elastic cross section.

The transport cross sections in all three sets were evaluated from the relationship

$$\sigma_j^{\text{tr}} = \sigma_j^{\text{t}} - \mu_j^{\text{el}} \sigma_j^{\text{el}}$$

$$\mu_j^{\text{el}} = \sigma_1^{\text{el}} / 3\sigma_0^{\text{el}}$$

where  $\sigma_j^{\text{tr}}$ ,  $\sigma_j^{\text{t}}$  and  $\sigma_j^{\text{el}}$  are the transport, total and elastic cross sections at group  $j$ ,  $\sigma_0^{\text{el}}$  and  $\sigma_1^{\text{el}}$  are the zeroth and first Legendre coefficients of elastic scattering in group  $j$ , and  $\mu_j^{\text{el}}$  is the average value of the cosine for elastic scattering in group  $j$ . This definition of  $\sigma^{\text{tr}}$  is based on the assumption that inelastic scattering is isotropic in the centre of mass and ignores the anisotropy in inelastic scatter in the laboratory frame.

The thorium data in all three sets were not corrected for resonance self shielding. This effect is negligibly small in the present investigation since the majority of the neutrons in the thorium assembly are above ~100 keV in the time interval of interest (~200 ns after the initial neutron pulse). For example, no resonance self shielding correction is given in the ABBN set

for energies above 100 keV and in the energy group 46.5 keV to 100 keV the correction is only ~2 per cent for the capture cross section.

The thorium data sets were not modified to account for the impurities in the thorium used in the measurements. The thin covering of cellulose acetate lacquer, of thickness in the range 0.013 to 0.025 mm, on each of the thorium bricks constituted the largest source of impurity. Calculations for a homogeneous mixture of thorium with 0.4 per cent of hydrogen have shown that the effect of the coating on the instantaneous decay constant is negligibly small in the case of the  $^{237}\text{Np}$  fission rate and generally less than 1.5 per cent in the case of the broad range detectors in the time range of interest.

Fission cross sections for  $^{237}\text{Np}$ ,  $^{235}\text{U}$  and  $^{239}\text{Pu}$  used in calculating detector responses were derived from both the ENDF/B-II and the UKNDL68 data files. The fission cross sections were group-averaged in the manner described for each of the thorium data sets.

#### 4. RESULTS OF CALCULATIONS

Figure 3a presents the calculated time dependent  $^{237}\text{Np}$  reaction rate associated with the fundamental mode for different combinations of  $^{232}\text{Th}$  data sets and  $^{237}\text{Np}$  fission cross section sets. Included in the same figure is the measured  $R_{111}$  mode. The measured reaction rate has been normalised at the peak to the calculation employing the ABBN thorium set and the UKNDL68 detector fission cross section set. The corresponding values of the theoretical and measured 'instantaneous decay constant',  $\lambda(t)$ , are shown in Figure 3b. The time channel widths used in the theoretical calculations were identical to those used in the experimental measurements, and the  $\lambda(t)$  were derived from the decay curves of the calculated fission rates by fitting the curves with a single exponential over the same number of time channels used in determining the experimental values of  $\lambda(t)$ .

The results for  $^{235}\text{U}$  and  $^{239}\text{Pu}$  are presented in Figure 4 and Figure 5 respectively.

#### 5. DISCUSSION

##### 5.1 The $^{237}\text{Np}$ Fission Rates

As clearly demonstrated in Figure 3, the calculated  $^{237}\text{Np}$  fission rates using the three thorium sets differ substantially from the experimental result and from each other. With the  $^{237}\text{Np}$  fission cross section from the same data file, the ABBN thorium set predicts a slower decay rate than either the UKNDL68 set or the ENDF/B-II set in the time interval of interest. Compared to the ENDF/B-II set, the UKNDL68 thorium set predicts a slower decay

rate at times less than ~90 ns after the peak of the time distributions and a faster decay rate at later times.

There is also a noticeable difference between calculations employing the UKNDL68 and the ENDF/B-II  $^{237}\text{Np}$  fission cross sections. The values of  $\lambda(t)$  using the two fission cross section sets differ from 0 to ~6 per cent in the time range of interest.

Near the peak of the time distributions all combinations of  $^{232}\text{Th}$  data sets and  $^{237}\text{Np}$  fission cross section sets predict a faster rate of decay than measured in the experiment. Away from the peak the measured  $R_{111}(t)$  and the associated  $\lambda(t)$  lie within the calculated curves. The short plateau observed in the experimental values of  $\lambda(t)$  between 40 ns and 65 ns after the peak of the curve is not evident in any of the calculations.

### 5.2 The $^{235}\text{U}$ and $^{239}\text{Pu}$ Fission Rates

The calculated  $^{235}\text{U}$  fission rates using various combinations of  $^{232}\text{Th}$  data and  $^{235}\text{U}$  fission cross section sets are in close agreement. This is also the case for the  $^{239}\text{Pu}$  fission rates. With the detector cross section for both  $^{235}\text{U}$  and  $^{239}\text{Pu}$  from the same data file, the ABBN  $^{232}\text{Th}$  data set predicts a slower decay rate at times before ~80 ns after the peaks of the time distributions and, later, a faster decay rate than either the UKNDL68 or the ENDF/B-II data sets. All three  $^{232}\text{Th}$  data sets predict too fast a decay rate for both the  $^{235}\text{U}$  and  $^{239}\text{Pu}$  fission rates compared to measurement for the first 80 ns or so after the peak; at later times the predicted values of  $\lambda(t)$  are close to the measured values. The oscillations which are evident in the measured  $^{239}\text{Pu}$  instantaneous decay constant from about 140 ns after the peak of the  $R_{111}(t)$  are not predicted by the calculations.

### 5.3 General

The discrepancies between the theoretical and experimental results can be ascribed broadly either to inadequacies in the calculational method and data used or to some systematic difference between the experimental and calculated parameters. An attempt has been made to keep such systematic differences to a minimum by feeding into the calculations much of the actual experimental conditions such as pulse width, pulse shape, source energy distribution, and detector jitter, and by processing the theoretical results in the same way as the experimental results. However, in the experiment it proved hard to determine the absolute time zero, that is the time at which neutrons were first generated at the target in the middle of the assembly. Since there is no asymptotic energy distribution in this fast neutron assembly, it is necessary to know the absolute time zero to compare properly the

experimental and theoretical results. In the absence of the knowledge of time zero, the time origin of the theoretical results was determined by assuming that the calculated fission rate corresponding to the  $R_{111}$  mode for a given detector peaks at the same time, with respect to the initial neutron pulse, as the measured  $R_{111}$  mode fission rate. That the technique is reasonable in the present situation, where the initial neutron pulses are short, and is unlikely to explain the discrepancy between theory and experiment, can be judged from the following observations:

- . Calculations indicate that the time at which the fission rate corresponding to the  $R_{111}$  mode peaks for a given initial neutron pulse is insensitive to the thorium data set used, since three data sets all predict the same peaking time for a given detector for the channel widths used in the present investigations.
- . Similarly, the peaking time is not very sensitive to the reaction rate since the  $^{237}\text{Np}$  fission rate peaks only  $\sim 1$  ns earlier than the non-threshold fission detectors.
- . Finally, the theoretical peaking times are insensitive, within the present timing accuracy, to changes in the pulse shape commensurate with the uncertainty in the measured pulse profile and the experimental ones to the number of modes used in the Fourier analysis.

This implies that the marked discrepancy observed between calculations and measurements is real, particularly at early times for the  $^{235}\text{U}$  or  $^{239}\text{Pu}$  fission rate, and must be attributed to deficiencies in the calculational method and/or errors in the cross section data used.

The errors in the thorium multigroup cross sections can come either from errors in the original point data or from inappropriate averaging of the point data when forming the group-averaged cross sections. It is clear, from the discrepancies between ENDF/B-II data and UKNDL68 data in Figure 2, that uncertainties exist in the point data for thorium. It is beyond the scope of this paper to assess the relative merits of the various point data, or to assess how much of the discrepancy between the theoretical and experimental parameters can be assigned to this error. However, Section 6 does examine the changes in the time dependent instantaneous decay constant for the various reaction rates following some well defined, physically reasonable changes in the group-averaged thorium data in different energy regions.

The group cross sections have been formed by averaging over spectra which are much more applicable to steady state problems than to time dependent

problems. Indeed, the correct method of averaging in these time dependent fast neutron assemblies presents a problem, since the neutron energy spectrum in these assemblies changes continuously with time. However, the comparatively fine group structure used, particularly in the case of the data sets derived from the UKNDL68 and ENDF/B-II files, and the fact that none of the cross sections vary rapidly in the energy region of interest, would lead one to expect that systematic errors would be small. Again the problem requires further study beyond the scope of this paper.

The differences in the calculations using the  $^{237}\text{Np}$  fission cross sections from the UKNDL68 and the ENDF/B-II files suggest some uncertainty in the  $^{237}\text{Np}$  fission cross sections. On the other hand, the predictions for the  $^{235}\text{U}$  and  $^{239}\text{Pu}$  fission rates are not very sensitive to the choice of the detector cross section sets. The ABBN, UKNDL68 and ENDF/B-II fission cross sections for  $^{235}\text{U}$  and  $^{239}\text{Pu}$  give values of  $\lambda(t)$  which differ generally by less than 3 per cent. Thus, any uncertainty in the  $^{235}\text{U}$  and  $^{239}\text{Pu}$  fission cross sections are not likely to be a major cause for the large discrepancy between theory and experiment at early times.

It seems likely that any major inadequacy of the present calculational technique lies in its inability to handle the space-energy dependence of the flux in the assembly. It should be recalled that the experimental technique is based on the fact that Fourier analysis of the measured space-time distributions is a well defined process, and the resulting fundamental mode can be compared unambiguously with the corresponding Fourier component of the calculated fission rates if the same characteristic length is used to Fourier analyse both distributions at any given time point. If this calculational technique is based on diffusion-asymptotic reactor theory then the Fourier mode is just the lowest mode of the calculation, provided the buckling is energy independent and the characteristic length used to calculate the buckling is the same as that used in the Fourier analysis. The reason for this is that, although space-time dependent reaction rates can be built up by summing the spatial modes of the diffusion theory calculation and so achieve, to some extent, the wave front-like properties of the pulse moving out from the source, subsequent Fourier analysis just retrieves the fundamental mode of the calculation.

The energy dependent buckling is tantamount to assuming energy independent boundary conditions and no coupling between the various spatial modes. Energy dependent boundary conditions could be taken into account to some extent by using group dependent bucklings similar to the scheme proposed by

Beynon (1971), but clearly we could then no longer compare the lowest mode with the experimental lowest Fourier mode. That this space-energy effect could be important at times close to the source can be gauged from the fact that the flight time of a 1 MeV neutron from the centre of the present assembly to the edge is  $\sim 14$  ns, which is significant compared to the total time range of interest of some 120 ns and instantaneous mean times  $(1/\lambda(t))$  of  $\sim 15$  ns.

It is also reasonable to expect, that, in the present geometry, diffusion theory will overpredict the instantaneous decay rate for neutrons close in time and energy to the source. At times after the end of the pulse the flux satisfies

$$\frac{1}{v} \frac{\partial \phi}{\partial t} + \text{div} \underset{\sim}{j} + \Sigma \phi - \int_0^{\infty} dE' \Sigma_s(E' \rightarrow E) \phi(E', r, t) = 0 \quad \dots (2)$$

Our Fourier analysis assumes that

$$\phi(r, E, t) = \Sigma \phi_n(E, t) \Psi_n(r)$$

where the  $\Psi(r)$  are a set of orthogonal functions which satisfy well defined boundary conditions (Ritchie and Moo 1974). Using the orthogonality of the  $\Psi(r)$  and Green's theorem we obtain for the fundamental mode

$$\begin{aligned} \frac{1}{v} \frac{\partial \phi_1}{\partial t} = & -\Sigma \phi_1 + \int_0^{\infty} dE' \Sigma_s(E' \rightarrow E) \phi_1(E', t) - \int_{\sim} dS \cdot \underset{\sim}{j} \\ & + \int d\tau \underset{\sim}{j} \cdot \text{grad} \Psi_1 \end{aligned} \quad \dots (3)$$

where  $\int_{\sim} dS$  denotes a surface integral and  $d\tau$  denotes a volume integral. Depending on the definition of the  $\Psi(r)$ , the third term on the right hand side of Equation (3) will be either identically zero or small. In the present geometry, with the source at the centre,  $\underset{\sim}{j} \cdot \text{grad} \Psi_1$  will be negative or zero over the whole range of the volume integral. If we define

$$\frac{\partial \phi_1}{\partial t} = \lambda_1(E, t)$$

$$\lambda_1(E, t) = v \Sigma \phi_1 - v \int dE' \Sigma_s(E' \rightarrow E) \phi_1(E') + v \int d\tau |\underset{\sim}{j} \cdot \text{grad} \Psi_1| \quad \dots (4)$$

Since diffusion theory does not adequately account for first flight neutrons, it will predict, in the present geometry, a flux distribution which is too peaked in the centre for neutrons with energies close to the source energy. Hence, it will predict a higher current than really exists at these energies and, from Equation (4), a higher instantaneous decay constant.

This argument could explain, in part, the high initial decay rates calculated for the  $^{237}\text{Np}$  fission rate which, with the present source conditions, could be considered to reflect the behaviour of neutrons with energies close to the source energies. It is not clear that the argument could be applied to the  $^{235}\text{U}$  and  $^{239}\text{Pu}$  fission rates which reflect the behaviour of a much broader spectrum of neutrons. Moreover, it would be reasonable to expect any errors due to the diffusion approximation to become small three or four mean scattering times away from the source. Since from 2 MeV to 200 keV the value of  $1/v\Sigma_{\text{tr}}$  in thorium is in the range 4 to 6.5 ns, we would expect the diffusion approximation to be quite good  $\sim 20$  ns after the pulse. Hence, it seems unlikely that the use of diffusion theory could explain the higher rates of decay which persist for  $\sim 60$  ns after the pulse for the calculated  $^{235}\text{U}$  and  $^{239}\text{Pu}$  decay rates and, for about the same time, for all the calculated  $^{237}\text{Np}$  decay rates with the exception of those predicted using the ABBN data set.

## 6. SENSITIVITY STUDIES

Figure 6 shows percentage changes in the instantaneous decay constant  $\lambda(t)$  of the  $^{237}\text{Np}$  and  $^{235}\text{U}$  fission rates for given changes in the group-averaged cross sections for the various neutron reactions in thorium derived from the ENDF/B-II file. In all cases, the calculations take account of both timing jitter and finite pulse length and derive  $\lambda(t)$  from fitting the decay curves with a single exponential. The behaviour of  $^{239}\text{Pu}$   $\lambda(t)$  is similar to that of  $^{235}\text{U}$  and has not been included.

In these studies it was assumed that the thorium total cross section was sufficiently well known that over the whole energy range it should be held constant when other cross sections are varied. It was also assumed that the elastic, fission and radiative capture cross sections were capable of independent measurement and that the total inelastic cross section at any energy was derived from the relationship

$$\sigma^{\text{inel}} = \sigma^{\text{t}} - (\sigma^{\text{el}} + \sigma^{\text{f}} + \sigma^{\text{n}\gamma}).$$

In the sensitivity studies only one of the independent cross sections  $\sigma^{\text{el}}$ ,

$\sigma^f$  or  $\sigma^{n\gamma}$  was modified at any one time and  $\sigma^{inel}$  was modified to keep  $\sigma^t$  constant. For example

$$m \sigma^{n\gamma} = (1 + \alpha) \circ \sigma^{n\gamma}$$

$$m \sigma^{inel} = \circ \sigma^{inel} - \alpha \circ \sigma^{n\gamma}$$

$$m \sigma_{g-g'}^{inel} = (1 - \alpha \circ \sigma_g^{n\gamma} / \circ \sigma_g^{inel}) \circ \sigma_{g-g'}^{inel}$$

where the superscript 'o' denotes the unmodified cross section and 'm' the modified cross section.

None of the  $\lambda(t)$  were sensitive within the present accuracy to changes in the thorium fission cross sections of up to 50 per cent. Similar changes in  $\sigma^{n\gamma}$  of ~20 per cent in the ranges 1 to 10 MeV and 0.33 to 1 MeV produced changes in the  $\lambda(t)$  of less than, or of the order of, 1 per cent which is below the sensitivity of the present experiments. However, it can be seen that the  $\lambda(t)$  are quite sensitive to changes in the elastic cross section and that changes of ~20 per cent in the elastic cross section produced changes of the order required to remove the discrepancies between the unmodified theory and experiment.

It can also be seen that changes in the cross sections affect the  $^{237}\text{Np}$   $\lambda(t)$  in a noticeably different way to the  $^{235}\text{U}$   $\lambda(t)$ . An increase of  $\sigma^{el}$  in the range 1 to 10 MeV and its consequent decrease in  $\sigma^{inel}$  increases the  $\lambda(t)$  of  $^{237}\text{Np}$  over the whole time range (~120 ns) during which the reaction rate is measured. The same change increases  $\lambda(t)$  of  $^{235}\text{U}$  only during the first 70 ns or so after the peak of the time distribution. Thereafter the change is negative, but quite small.

The increase in  $\sigma^{el}$  has two effects. It decreases the inelastic cross section and decreases the transport cross section. At high energies, to which the  $^{237}\text{Np}$  fission detector is sensitive the changes will have opposite effects since a decrease in  $\sigma^{inel}$  decreases the removal rate at a given energy while a decrease in  $\sigma^{tr}$  increases the leakage rate. It is evident that, at high energies, leakage is more important than removal by inelastic scatter in this assembly. Since the  $^{235}\text{U}$  is sensitive to a broad range of neutron energies a change in the inelastic cross sections will affect  $\lambda(t)$  through a change in spectrum since neutrons are not in fact removed from the system. A decrease in  $\sigma^{inel}$  would tend to harden the spectrum at early times so that the changes in the  $^{235}\text{U}$   $\lambda(t)$  due to the changes in  $\sigma^{tr}$  or  $\sigma^{inel}$

would be in the same direction. However, the change should not extend over a long time range as the behaviour of high energy neutrons should dominate the reaction rate for only a short period after the end of the pulse. This is consistent with the behaviour in Figure 6b. The lower  $\lambda(t)$  in  $^{235}\text{U}$  at longer times could be ascribed to a diffusion cooling effect.

It is interesting to note that increasing  $\sigma^{el}$  between 0.33 to 1 MeV by 20 per cent decreases  $\lambda(t)$  for  $^{237}\text{Np}$  over much of the present range of measurement by ~5 to 10 per cent, but increases the  $\lambda(t)$  of  $^{235}\text{U}$  by about the same amount over much of its time range of measurement. The change in the  $^{235}\text{U}$   $\lambda(t)$  can be explained using arguments similar to those used above. In the case of the  $^{237}\text{Np}$   $\lambda(t)$  the decreased removal rate between 1 MeV and 0.33 MeV due to the decreased  $\sigma^{inel}$  more than compensates for the increased leakage. The effect of this change on the  $^{235}\text{U}$  fission rate at times greater than ~200 ns is quite small, which is to be expected since by that time after the source most of the neutrons have been slowed down past 300 keV.

It should be stressed that these sensitivity studies were done to indicate how sensitive the measured parameters were to physically reasonable changes in thorium cross sections rather than to point out deficiencies in the nuclear data for thorium. It would appear that the parameters are insensitive to  $\sigma^{n\gamma}$  and  $\sigma^f$ , but changes of ~10 per cent or perhaps 5 per cent in  $\sigma^{el}$  produced systematic changes in  $\lambda(t)$  which should be discernible from the experimental results. It would be inadvisable to use the present results as a basis for modifying the thorium cross sections. The energy range over which the changes were made was chosen almost arbitrarily. The fact that the changes in  $\sigma^{el}$  above 1 MeV change  $\lambda(t)$  for both  $^{237}\text{Np}$  and  $^{235}\text{U}$  in the same direction, but similar changes between 0.33 MeV and 1 MeV change the  $\lambda(t)$  in opposite directions stresses the need for further sensitivity studies and also further experiments with different detectors and different source conditions.

#### 7. ACKNOWLEDGEMENTS

We wish to thank Mr. H.D. Ferguson for preparing the thorium data sets from the ENDF/B-II and WINFRITH files. One of us, S.P. Moo, is very grateful to the Colombo Plan (Australia) for a post-graduate scholarship, to the Australian Institute of Nuclear Science and Engineering for its generous grant to the University of Tasmania in support of this work and to Drs. K.B. Fenton and A.G. Fenton of the University of Tasmania for their continued interest and support.

8. REFERENCES

- Argonne National Laboratory (1963) - ANL-5800 (2nd ed.).
- Bondarenko, I.I. (1964) - 'Group Constants for Nuclear Reactor Calculations'.  
Consultants Bureau, New York.
- Clancy, B.E. (1969) - AAEC Local Code, private communication.
- Doherty, G. (1968) - AAEC Local Code, private communication.
- Inada, T., Kawachi, K. and Hiramoto, T. (1968) - J. Nucl. Sci. and Technol.  
5, 22.
- Maher, K.J., Ritchie, A.I.M. and Rainbow, M.T. (1967) - Proc. IAEA Symp.  
Neutron Thermalisation and Reactor Spectra, Vol.2, p.245.
- Moo, S.P., Rainbow, M.T. and Ritchie, A.I.M. (1973) - AAEC/E254; also  
J. Nucl. Energy (In press).
- Norton, D.S. (1968) - AAEW-M824.
- Ritchie, A.I.M. and Moo, S.P. (1974) - to be published.
- Whittlestone, S. (1972) - private communication.
- Wright, R.Q., Greene, N.M., Lucius, J.L. and Craven Jr., C.W. (1969) -  
ORNL-TM-2679.



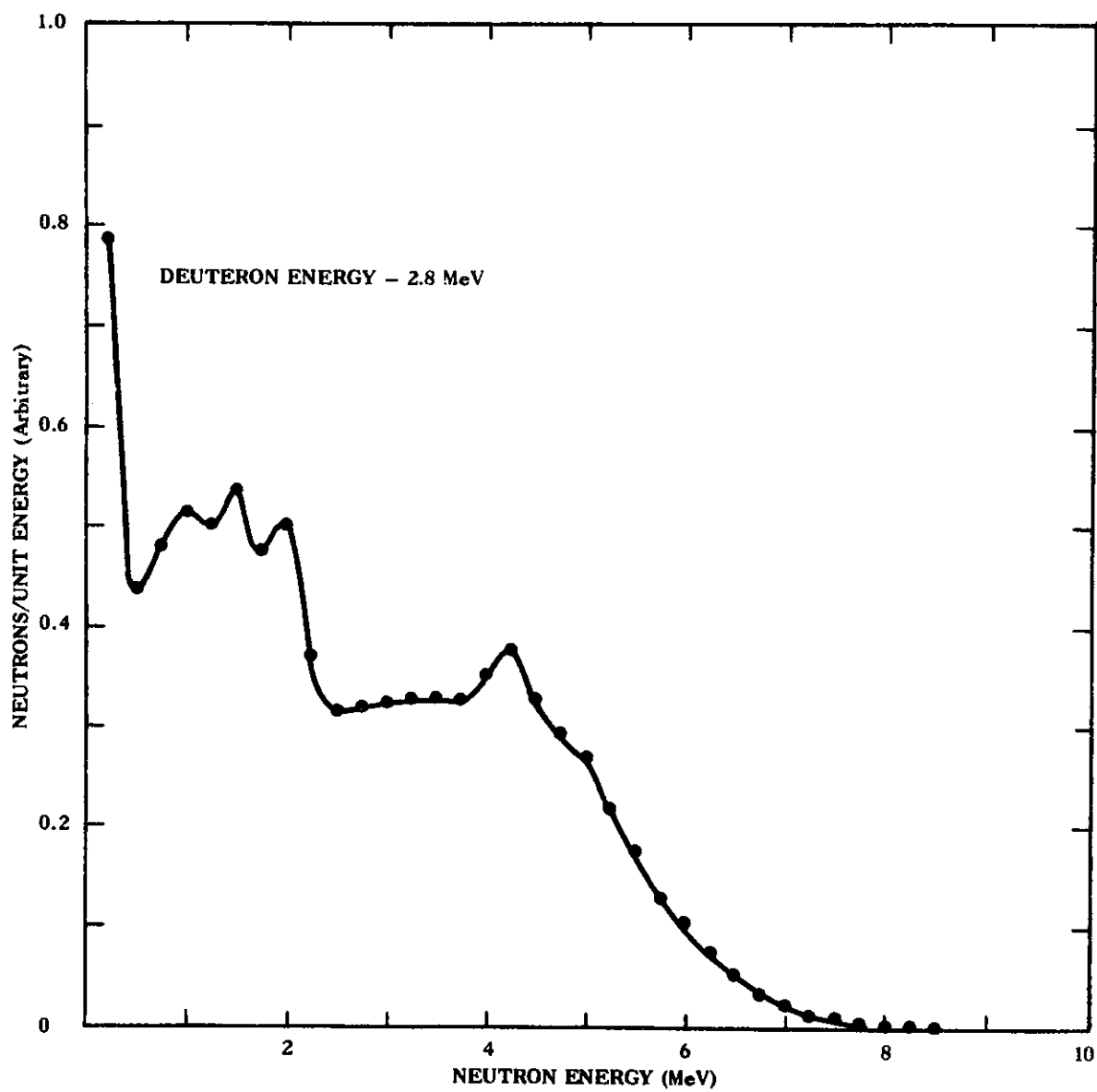


FIGURE 1 ANGLE INTEGRATED NEUTRON ENERGY SPECTRUM FROM THE  ${}^9\text{Be}(d,n){}^{10}\text{B}$  THICK TARGET REACTION

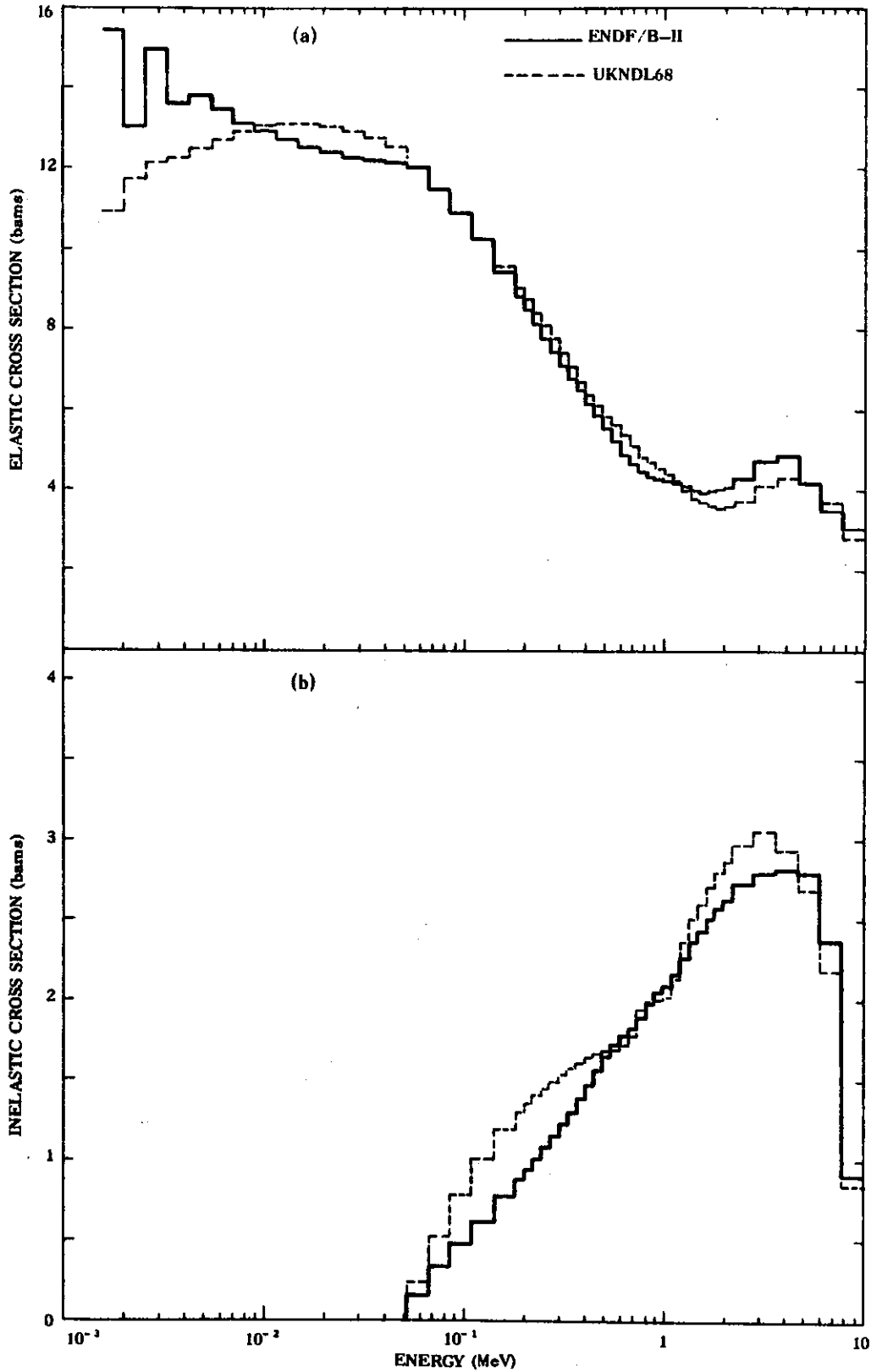


FIGURE 2 THE GROUP AVERAGED (a) ELASTIC AND (b) INELASTIC CROSS SECTIONS FOR THORIUM DERIVED FROM THE UKNDL68 AND ENDF/B-II DATA FILES

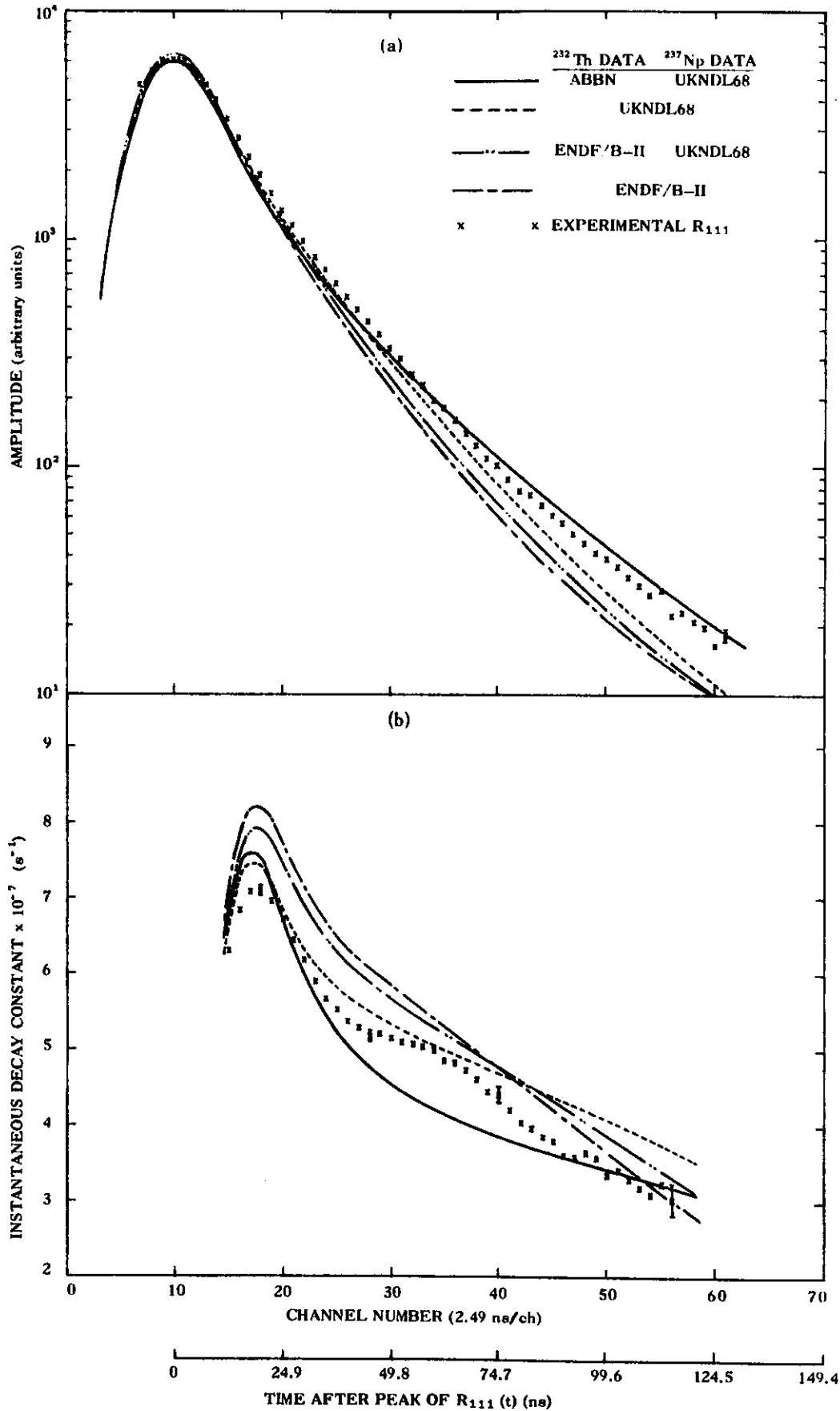


FIGURE 3 THEORETICAL AND EXPERIMENTAL VALUES OF THE FUNDAMENTAL MODE FISSION RATES FOR  $^{237}\text{Np}$  AS A FUNCTION OF TIME. (a) THE FUNDAMENTAL MODE TIME DISTRIBUTION. (b) THE INSTANTANEOUS DECAY CONSTANT  $\lambda(t)$

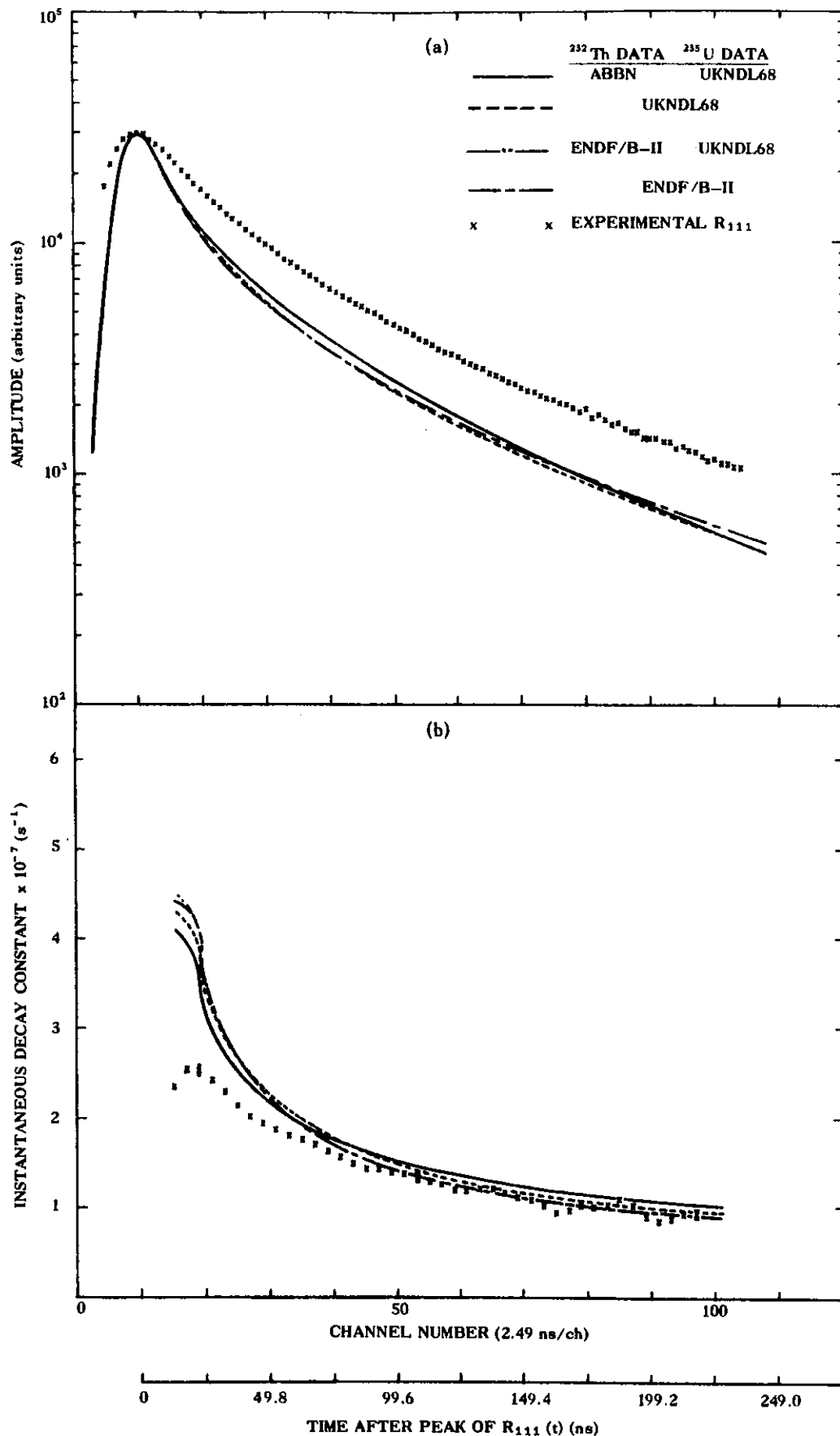


FIGURE 4 THEORETICAL AND EXPERIMENTAL VALUES OF THE FUNDAMENTAL MODE FISSION RATES FOR  $^{235}\text{U}$  AS A FUNCTION OF TIME. (a) THE FUNDAMENTAL MODE TIME DISTRIBUTION. (b) THE INSTANTANEOUS DECAY CONSTANT  $\lambda(t)$

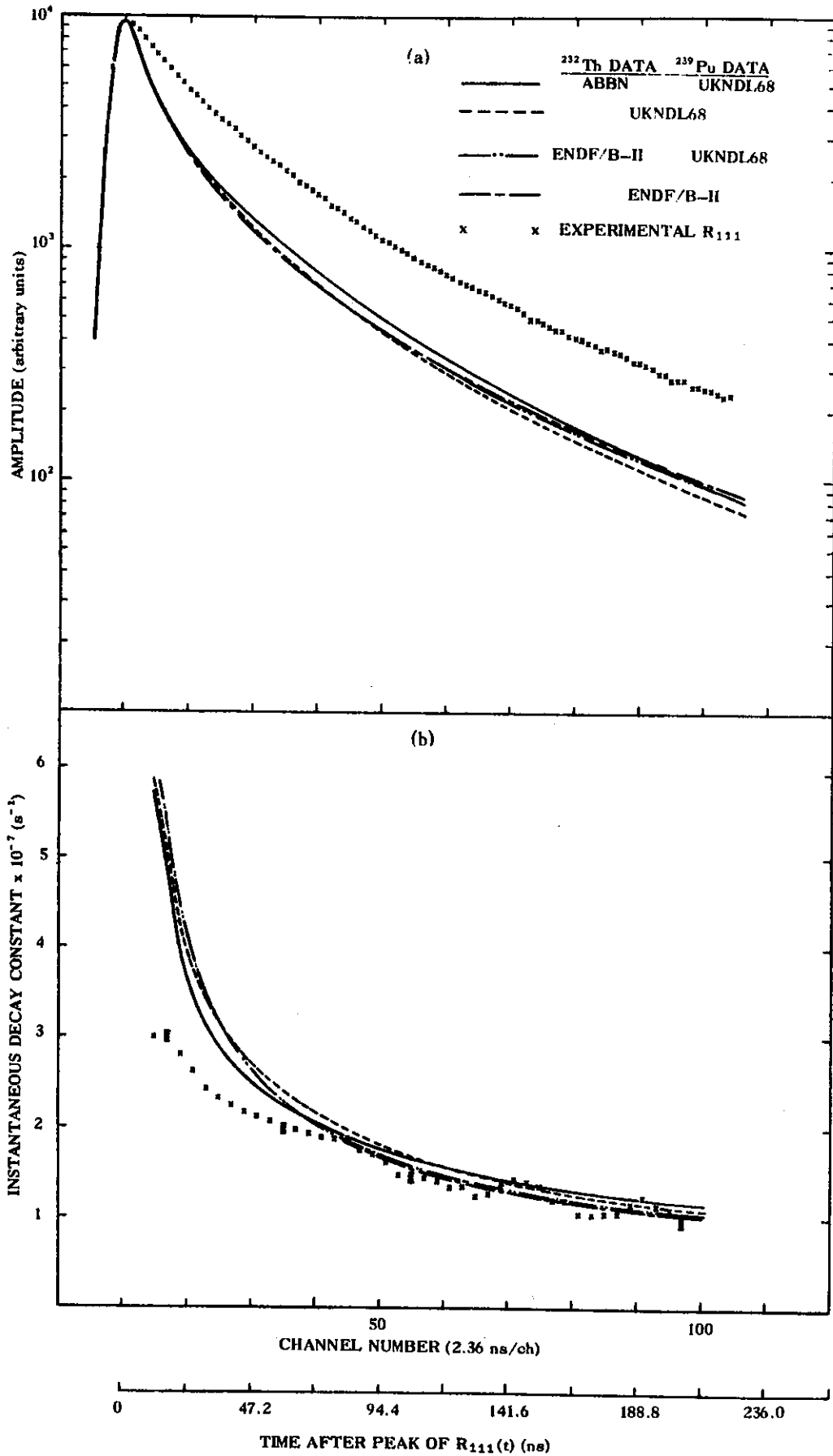


FIGURE 5 THEORETICAL AND EXPERIMENTAL VALUES OF THE FUNDAMENTAL MODE FISSION RATES FOR  $^{239}\text{Pu}$  AS A FUNCTION OF TIME. (a) THE FUNDAMENTAL MODE TIME DISTRIBUTION. (b) THE INSTANTANEOUS DECAY CONSTANT  $\lambda(t)$

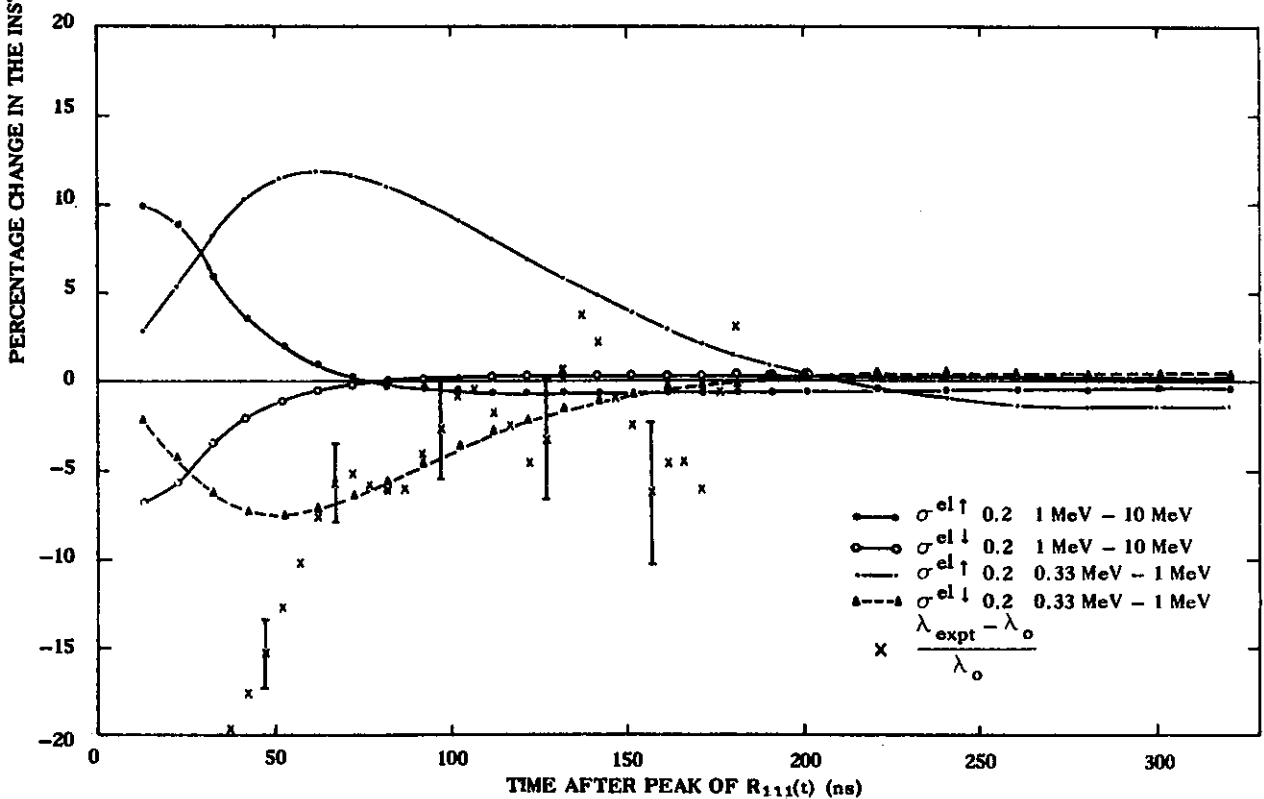
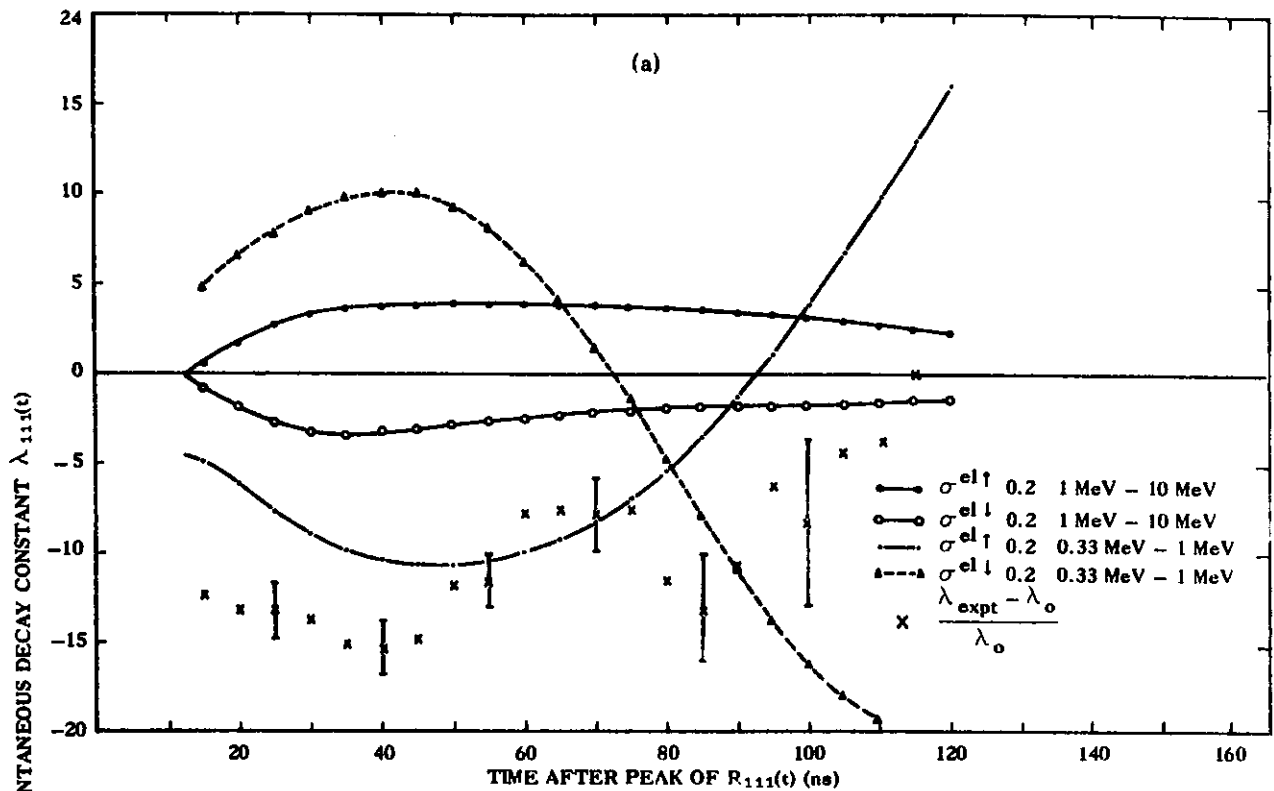


FIGURE 6 PERCENTAGE CHANGES IN THE INSTANTANEOUS DECAY CONSTANT  $\lambda(t)$  OF (a)  $^{237}\text{Np}$  AND (b)  $^{235}\text{U}$  FISSION RATES FOR GIVEN CHANGES IN THE THORIUM GROUP-AVERAGED ELASTIC CROSS SECTION